Antiretroviral therapy duration and immunometabolic state determine efficacy of *ex vivo* dendritic cell-based treatment restoring functional HIV-specific CD8+ T cells in people living with HIV

Marta Calvet-Mirabent,[a,b] Ildefonso Sánchez-Cerrillo,[a,b] Noa Martín-Cófreces,[a,b,c] Pedro Martínez-Fleta,[a] Hortensia de la Fuente,[a,c] Ilya Tsukalov,[b] Cristina Delgado-Arévalo,[a,b] María José Calzada,[b] Ignacio de los Santos,[d,g] Jesús Sanz,[d,g] Lucio García-Fraile,[d,g] Francisco Sánchez-Madrid,[a,b,c] Arantzazu Alfranca,[a] María Ángeles Muñoz-Fernández,[e] Maria J. Buzón,[f] and Enrique Martín-Gayo [a,b,g]*

[a]Immunology Unit from Hospital Universitario de La Princesa and Instituto de Investigación Sanitaria Princesa, Madrid, Spain
[b]Universidad Autónoma de Madrid, Madrid, Spain
[c]Centro de Investigación Biomédica en Red Cardiovascular, CIBERCV, 28029 Madrid, Spain
[d]Infectious Diseases Unit from Hospital Universitario de La Princesa, Madrid, Spain
[e]Immunology Section, Instituto de Investigación Sanitaria Gregorio Marañón (IiSGM), Hospital General Universitario Gregorio Marañón, Madrid, Spain
[f]Infectious Diseases Department, Institut de Recerca Hospital Univesritari Vall d'Hebrón (VHIR), Universitat Autònoma de Barcelona, Barcelona, Spain
[g]Centro de Investigación Biomédica en Red Infecciosas, CIBERINF, 28029 Madrid, Spain

eBioMedicine 2022;81: 104090
Published online 2 June 2022
https://doi.org/10.1016/j.ebiom.2022.104090

Summary

Background Dysfunction of $CD8^+$ T cells in people living with HIV-1 (PLWH) receiving anti-retroviral therapy (ART) has restricted the efficacy of dendritic cell (DC)-based immunotherapies against HIV-1. Heterogeneous immune exhaustion and metabolic states of $CD8^+$ T cells might differentially associate with dysfunction. However, specific parameters associated to functional restoration of $CD8^+$ T cells after DC treatment have not been investigated.

Methods We studied association of restoration of functional HIV-1-specific $CD8^+$ T cell responses after stimulation with Gag-adjuvant-primed DC with ART duration, exhaustion, metabolic and memory cell subsets profiles.

Findings HIV-1-specific $CD8^+$ T cell responses from a larger proportion of PLWH on long-term ART (more than 10 years; LT-ARTp) improved polyfunctionality and capacity to eliminate autologous $p24^+$ infected $CD4^+$ T cells *in vitro*. In contrast, functional improvement of $CD8^+$ T cells from PLWH on short-term ART (less than a decade; ST-ARTp) after DC treatment was limited. This was associated with lower frequencies of central memory $CD8^+$ T cells, increased co-expression of PD1 and TIGIT and reduced mitochondrial respiration and glycolysis induction upon TCR activation. In contrast, $CD8^+$ T cells from LT-ARTp showed increased frequencies of $TIM3^+$ $PD1^-$ cells and preserved induction of glycolysis. Treatment of dysfunctional $CD8^+$ T cells from ST-ARTp with combined anti-PD1 and anti-TIGIT antibodies plus a glycolysis promoting drug restored their ability to eliminate infected $CD4^+$ T cells.

Interpretation Together, our study identifies specific immunometabolic parameters for different PLWH subgroups potentially useful for future personalized DC-based HIV-1 vaccines.

Funding NIH (R21AI140930), MINECO/FEDER RETOS (RTI2018-097485-A-I00) and CIBERINF grants.

Keywords: HIV; $CD8^+$ T cell; Dendritic cell; Immunotherapy; Immune exhaustion; Metabolism

*Corresponding author at: Universidad Autónoma de Madrid; Medicine Department, Immunology Unit, Hospital Universitario de La Princesa; Calle de Diego de León, 62, 28006 Madrid, Spain. Tel.: +34 915 2023 07, Fax: +34 915 2023 74.
E-mail address: enrique.martin@uam.es (E. Martín-Gayo).

Research in context

Evidence before this study

Current antiretroviral therapies available for people living with HIV-1 (PLWH) are unable to eliminate persistently infected $CD4^+$ T cells and eradicate the infection. For this reason, different immunotherapeutic strategies aiming to boost antiviral immunity and to reduce HIV-1 reservoirs have been tested during the last decade. However, none of these immunotherapies have been effective and prevented viral rebound after treatment interruption in clinical trials. Such negative results are in part due to heterogeneous dysfunctional states in immune cells with antiviral activity, such as $CD8^+$ T cells. Thus, it is critical to better understand mechanisms regulating functionality of $CD8^+$ T cells to develop personalized strategies to more efficiently reinvigorate the function of these immune cells and to reduce HIV-1 reservoirs.

Added value of this study

We identified two subgroups of PLWH characterized by significant differences in $CD8^+$ T cell immunometabolic phenotypes and their ability to respond to adjuvant-primed dendritic cell (DC) immunotherapy. $CD8^+$ T cells capable of improving cytotoxic activity against HIV-1 infected cells after DC immunotherapy, were enriched for PLWH in treatment for more than a decade, exhibited low levels of co-expression of PD1 and TIGIT checkpoint inhibitory receptors, and preserved metabolism and memory cell subsets. In contrast, dysfunctional $CD8^+$ T cells unable to respond to adjuvant-activated DC therapy were enriched with PLWH in treatment for less than ten years, displaying high proportions of $PD1^+$ $TIGIT^+$ cells and reduced mitochondrial fitness. We were able to restore functionality of $CD8^+$ T cells from this group by combining DC therapy with the use of blocking antibodies against PD1 and TIGIT combined with the glycolysis-promoting drug Metformin.

Implications of all the available evidence

Our study identifies specific groups of PLWH with a higher probability of responding to dendritic cell immunotherapy, key CD8+ T cell patterns differentially contributing to immune dysfunction and validates new approaches to restore the function of dysfunctional cells from non-responding individuals. Therefore, these data might provide new tools to improve and personalize these treatments in PLWH characterized by elevated levels of immune exhaustion and metabolic dysfunction and increase efficacy of immunotherapies against HIV-1 infection.

Introduction

Antiretroviral therapy (ART) does not eradicate chronic HIV-1 infection due to persistent HIV-1 reservoir cells maintained through homeostatic proliferation of long-lived latently infected memory $CD4^+$ T cells, residual viral replication in tissues and dysfunctionality of the immune response.[1-4] Therefore, additional strategies to eradicate the latent reservoir are required. Strategies directed to improve viral reactivation of latently HIV-1 infected cells and the use of immunotherapy to boost their elimination by immune cytotoxic cell subsets have been investigated.[5,6] Cytotoxic $CD8^+$ T lymphocytes are immune cells crucial for restraining the size of the reservoir in the initial phases of the infection[7] and for natural control of HIV-1 replication in elite controller (EC) individuals.[8] Several therapeutic strategies have focused on enhancing the magnitude and polyfunctionality of HIV-1-specific $CD8^+$ T cell responses in people living with HIV-1 (PLWH)[8,9] to mimic the effective and durable immune responses of EC.[10] However, none of the tested candidates prevented viral rebound following treatment interruption in clinical trials.[11,12] Thus, new personalized strategies that take into consideration complex factors contributing to $CD8^+$ T cell dysfunction are needed.

A potential strategy is to improve antigen-presenting cell function of dendritic cells (DC), which could be compromised in PLWH.[13] Previous studies on HIV-1 infected EC identified a DC activation state dependent on the TANK-Binding Kinase 1 (TBK-1) which is characterized by highly functional capacities to activate polyfunctional HIV-specific $CD8^+$ T cell responses.[14,15] TBK-1 is a master regulator downstream of multiple intracellular nucleic acid sensors, which leads to the production of type I and II interferons.[16] We previously showed that activation of DC through agonists of nucleic acid sensors upstream of TBK-1 potentiate the acquisition of EC-like functional profiles and their ability to increase polyfunctional HIV-1-specific $CD8^+$ T cell responses in lymphoid tissues in humanized mice.[17] Also, DC might be intrinsically useful to more efficiently reactivate the latent HIV-1 reservoir.[18,19]

On the other hand, basal hyperactivation and immune exhaustion compromise the maintenance and effector function of HIV-1 specific $CD8^+$ T in PLWH.[20-23] Recent studies have shown that exhaustion of $CD8^+$ T cells is a dynamic process involving expression of multiple checkpoint inhibitory receptors that drive the transition, survival and function of distinct memory cell subsets.[22,24,25] Importantly, expression of checkpoint inhibitory receptors such as Programmed cell death protein 1 (PD1), T cell immunoreceptor with Ig and ITIM domains (TIGIT) and T cell immunoglobulin and mucin domain-containing protein 3 (TIM3) in T cells is also associated with deregulated glucose metabolism,[26-28] potentially affecting the effector function and longevity of HIV-1-specific $CD8^+$ T cells.[29-31] Consistently, compromise of metabolic fitness has been reported in PLWH and suggested to affect $CD8^+$ T cell function.[32,33] In addition, prolonged ART might restore some of these defects and facilitate post-treatment immunological control of

viral replication.[34,35] However, it is unknown whether specific expression patterns of checkpoint inhibitory receptors might differentially associate with efficacy of DC immunotherapy restoring functionality of HIV-1-specific CD8$^+$ T cells in PLWH on ART.

Here, we evaluated the efficacy of adjuvant-primed DC reinvigorating polyfunctional and cytotoxic HIV-1-specific CD8$^+$ T cells, and its association with the immunometabolic state in different subgroups of PLWH at different times since ART initiation. We report enhanced response of CD8$^+$ T cells to DC treatment in PLWH on ART for more than a decade, which associates with higher central memory (CM) frequencies, enrichment on TIM3$^+$ PD1$^-$ cells and the ability to induce glycolysis upon TCR stimulation. In contrast, CD8$^+$ T cells from PLWH under ART for less than 10 years were characterized by decreased frequency of CM, increased proportions of exhausted PD1$^+$ TIGIT$^+$ memory CD8$^+$ T cells, impaired glycolytic metabolism and inability to reinvigorate cytotoxic function of CD8$^+$ T cells after DC stimulation. Importantly, combined blockade of PD1 and TIGIT receptors and the use of the pro-glycolytic drug Metformin more consistently restored cytotoxic capabilities of dysfunctional CD8$^+$ T cells from PLWH. Collectively, our study uncovers immunometabolic parameters associated with response of CD8$^+$ T cells to DC-based HIV-1 vaccine in PLWH, which might be useful for future personalized treatments.

Methods

Experimental design

Peripheral blood mononuclear cells (PBMC) were isolated from n=49 PLWH on ART with clinical characteristics summarized in Table 1, provided by the Infectious Diseases Unit from Hospital de La Princesa, Madrid, Spain. N=12 HIV negative donors were provided either by the Immunology Service from Hospital de La Princesa or Centro de Transfusión of Comunidad de Madrid, Spain (Table 2). Samples were cryopreserved upon collection and used in parallel in our study.

Ethics statement

All participating subjects received and signed an informed consent, approved by the Ethics committee from Hospital Universitario de La Princesa (Register Number 3518), following the Helsinki declaration. We tried to include the same donors in all the analyses but in some cases, this was not possible due to sample availability. Number of individuals from our cohort used for each experiment is specified on the figure legends. The study was designed in accordance with the STROBE guidelines (see supplementary STROBE checklist and Figure 1).

DC generation and *in vitro* stimulation

Monocyte-derived DCs (MDDCs) were generated from circulating monocytes enriched by adherence and cultured in RPMI 1640 media supplemented with 10% Fetal Bovine Serum (HyClone) in the presence of 100 IU/mL of GM-CSF and 100 IU/mL of IL4 (Peprotech) for 6 days. Subsequently, MDDCs were harvested and cultured over-night in media alone or in the presence of 5 μg/mL of a pool of 15-mer overlapping HIV-1 Gag peptides provided by the NIH AIDS Reagent Program (#11057) either individually or in combination with 1 μg/mL of 2'3'-c'diAM(PS)2 (Invivogen) STING agonist and 2.5 μg/mL of Poly I:C (SIGMA) TLR3 ligand as adjuvant treatment. Maturation of MDDC after treatment with Gag-peptides and/or adjuvants was assessed by flow cytometry analysis of CD40 expression (see *Flow cytometry*).

Isolation of human peripheral blood T lymphocyte populations

Total or individual CD8$^+$ or CD4$^+$ T cells were purified from PBMC suspensions from our PLWH and HIV-1 negative control study cohorts by negative immunomagnetic selection (purity >90%) using the Untouched Human T cell and CD4 T cell Dynabeads Kits (Invitrogen) and the MojoSort Human CD8 T cell (BioLegend) isolation kits. Memory CD45RA$^-$ CD8$^+$ T cells from PLWH and HIV-1 negative controls were isolated from CD8+ T cells by negative immunomagnetic selection after treatment with mouse anti-human CD45RA mAbs (Biolegend) and Goat anti-Mouse IgG covered Dynabeads (Invitrogen).

In vitro activation of HIV-1 specific CD8$^+$ T cells from PLWH

MDDCs pre-treated with media only or either with HIV-1 Gag peptides alone or incubated with the adjuvants, were co-cultured with purified autologous T cells in a 1:5 ratio. After 5 h incubation of MDDC and autologous T cells, 0.25 μg/mL Brefeldin A (SIGMA), 0.0025 mM Monensin (SIGMA) and 0.2 μg/mL anti-CD107a-APC antibody (Biolegend) were added to the media and then cultured over-night. Analysis of total IFNγ expression and co-expression with CD107a (polyfunctionality) in CD8$^+$ T cells was performed by flow cytometry.

In vitro analysis of CD8$^+$ T cells functionality

CD4$^+$ T cells were purified from PLWH, stained with 5 μM violet cell trace tracker (Invitrogen), and cultured in the presence of 30 μM Raltegravir (Selleck Chemicals) alone, to prevent new rounds of infections in culture, or in combination with 50 nM Romidepsin (Selleck Chemicals), as a latency reversal agent, in the absence or the presence of autologous CD8$^+$ T cells

	Total HIV chronic patient cohort	ST-ARTp	LT-ARTp	p-values
Patient cohort individuals (n)	49	31	18	
Age at sample collection Median (1^{st}- 3^{rd} quartile); stdev p	48 (39-56); 12	40 (37-51); 9	55.5(51-67); 10	<0.0001
Sex M: male (%); F: female (%)	M: 42 (86%);F: 7 (14%)	M: 30 (97%);F: 1(3%)	M: 12 (67%);F: 6 (33%)	0.013
NADIR circulating $CD4^+$ T cell countsMedian (1^{st}- 3^{rd} quartile); stdev p	420 (265-504);222.292 ND	480.5(340-555); 219.861 ND	318 (117-434); 171.441 ND	0.0039
Circulating $CD4^+$ T cell counts at sample collectionMedian (1^{st}- 3^{rd} quartile); stdev p	866 (659-1194); 3301 ND	1016 (728-1277); 3571 ND	777(634-1086); 225	0.039
Circulating $CD8^+$ T cell counts at sample collectionMedian (1^{st}- 3^{rd} quartile); stdev p	900 (651-1350); 489 1 ND	993(684-1400); 527 1ND	833(525-1301); 383	ns
$CD4^+$/$CD8^+$ T cell ratio in the blood at sample collection Median (1^{st}- 3^{rd} quartile); stdev p	1.00 (1-1); 0.46 1 ND	1.06(1-1); 0.41 1 ND	0.97(1-1); 0.53	ns
BLIPS 0: patients (%); 1: patients (%); ND: patients (%)	0: 34 (69.4%); 1: 8 (16.3%); ND: 7 (14.3%)	0: 23 (74%); 1: 5 (16%); ND: 3 (10%)	0: 11 (61%); 1: 3 (17%); ND: 4 (22%)	ns
Years under treatment Median (1^{st}- 3^{rd} quartile); stdev p	8 (4-15); 6	5.5 (3-8); 3	15(14-19); 3	<0.0001
Months from HIV detection to ART initiation Median (1^{st}- 3^{rd} quartile); stdev p	1ss); 51.57	3 (0-66); 44.23	22.5(1-99); 61.35	ns
Treatment [number of patients]	ABC/3TC/DTG [9]; ABC/3TC/LPV/r [1]; DRV/c [6]; DRV/c/DTG/3TC [1]; DRV/c/TDF/AZT [1]; DRV/RPV/FTC [1]; DTG/RPV [1]; DTG/3TC [2]; TAF/FTC/BIC [5]; TAF/FTC/DRV/c [9]; TAF/FTC/DRV/c/DTG [1]; TAF/FTC/EVG/c [5]; TAF/FTC/RPV [2]; TAF/FTC/NVP [1]; TDF/FTC/EFV [4]	ABC/3TC/DTG [6]; ABC/3TC/LPV/r [0]; DRV/c [2]; DRV/c/DTG/3TC [0]; DRV/c/TDF/AZT [1]; DRV/RPV/FTC [0]; DTG/RPV [1]; DTG/3TC [2]; TAF/FTC/BIC [5]; TAF/FTC/DRV/c [6]; TAF/FTC/DRV/c/DTG [0]; TAF/FTC/EVG/c [3]; TAF/FTC/RPV [2]; TAF/FTC/NVP [0]; TDF/FTC/EFV [3]	ABC/3TC/DTG [3]; ABC/3TC/LPV/r [1]; DRV/c [4]; DRV/c/DTG/3TC [1]; DRV/c/TDF/AZT [0]; DRV/RPV/FTC [1]; DTG/RPV [0]; DTG/3TC [0]; TAF/FTC/BIC [0]; TAF/FTC/DRV/c [3]; TAF/FTC/DRV/c/DTG [1]; TAF/FTC/EVG/c [2]; TAF/FTC/RPV [0]; TAF/FTC/NVP [1]; TDF/FTC/EFV [1]	

***Table 1*: Clinical characteristics of ART-treated HIV-1 chronic patient cohort.**
*ND = non determined.
Statistical significances were calculated using two-tailed Wilcoxon test and Chi-square test with Yates correction.

treated with MDDC pre-treated under different conditions at a 2:1 ratio.

In some functional experiments, we evaluated the impact of blocking different checkpoint inhibitory receptors and/or stimulating glycolysis in $CD8^+$ T cells during co-culture with the activated MDDCs. In these assays, media was supplemented with 2 μg/mL of mouse IgG1 K anti-human PD-1 antibody (Biolegend) either alone

		p-values *vs.*		
		Total ART (all; metab)	ST-ARTp (all; metab)	LT-ARTp (all; metab)
Healthy control cohort individuals (n)	12			
Age at simple collection Median (1^{st}- 3^{rd} quartile); stdev p	45.5(28-57.75); 15	0.6966; 0.5074	0.4571; 0.4658	0.0335; 0.0567
Sex M: male (%); F: female (%)	M: 7 (64%); F: 4 (36%)	0.2009; 0.5705	0.0176; 0.3661	0.8134; 0.8772

***Table 2*: HIV negative donor cohort.**
*metab = samples used for metabolism assays.
Statistical significances were calculated using two-tailed Wilcoxon test and Chi-square test with Yates correction.

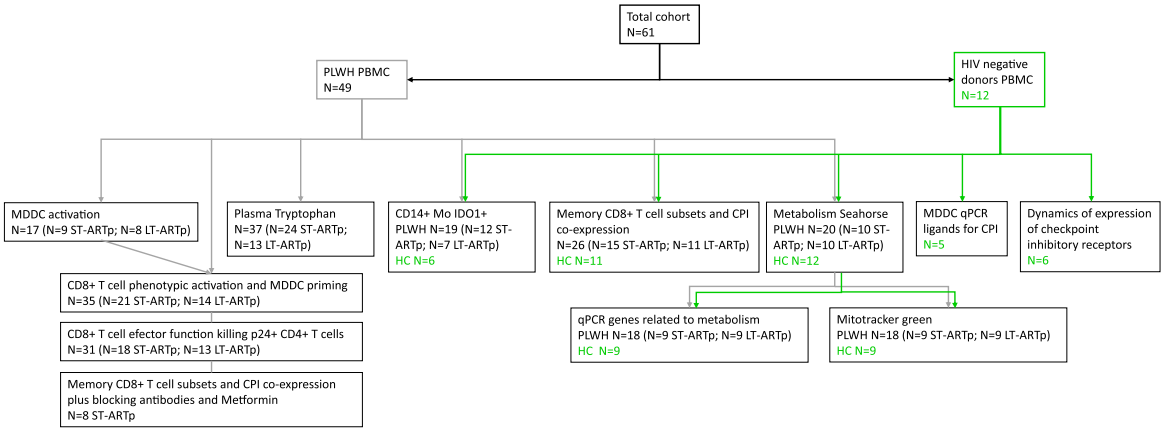

Figure 1. STROBE flow chart. Flow chart indicating the number of donors used for each assay. PLWH are indicated in dark grey and HIV negative controls in green.

or in combination with 1 μg/mL mouse IgG2 B anti-human TIGIT (R&D systems) or 1 μg/mL goat IgG anti-human TIM-3 (R&D systems) and alone or in combination of 5 mM Metformin (SIGMA) consistent with concentration ranges used in previous studies.[36-39] As a control, we used corresponding isotype control antibodies (mouse IgG1 K and mouse IgG2 B, both from Biolegend; goat IgG from SIGMA) and Metformin's carrier.

Flow cytometry and fluorometric analyses

Analysis of cell viability *ex vivo* or after culture was performed using APC-H7 (Tonbo Biosciences) or LIVE/DEAD Fixable Yellow 405 (Invitrogen) viability dye, in the presence of different panels of monoclonal antibodies. Clones, fluorochromes and commercial information of antibodies used are detailed in Supplementary Table 1. For analysis of MDDC activation we used mAbs against lineage markers (CD3, CD19, CD56), CD11c, CD40, and HLA-DR. For analysis of *in vitro* activation of HIV-1 specific $CD8^+$ T cell responses, anti-human CD3, CD8, CD107a and IFNγ mAbs were used. For functional assays with $CD8^+$ T cells anti-human CD3, CD4, CD8, and anti-HIV-1 p24 mAbs were used. $CD8^+$ T cell memory and exhaustion phenotypes were defined using anti-human CD3, CD8, CD45RO, PD1, TIGIT, TIM3, and CCR7 mAbs. PBMC from PLWH and HIV-1 negative individuals were also stained using a combination of anti-CD3, CD8, CD11c, CD14, HLA-DR mAbs and intracellular anti-IDO-1 mAb. Samples were analysed on a FACS Canto II cytometer (BD Biosciences). Analysis of individual and Boolean multiparametric flow cytometry data was performed using FlowJo v10.6 software (Tree Star).

Fluorometric quantification of tryptophan levels in plasma from PLWH was performed using the Tryptophan Assay kit (Abcam), following manufacturer's instruction, and analysed with a GloMax Discover instrument (Promega).

RNA extraction and qPCR mRNA quantification

Total RNA was isolated using the RNeasy Micro Kit (Qiagen) either from MDDCs from HIV-1 negative donors or from memory $CD45RA^-$ $CD8^+$ T cells from PLWH and HIV-1 negative controls. cDNA was then synthesized and transcriptional levels of PD-L1, CD155 and Gal-9 on MDDC, and HIF1α, GLUT1, PDK1 and GAPDH on memory CD8 T cells were quantified by qRT-PCR. Primers sequences are detailed in Supplementary Table 2. Amplifications were performed in a StepOne Plus Real time PCR system (Applied Biosystems). Finally, relative mRNA expression was determined after normalization of each transcript to endogenous β-actin expression.

Analysis of metabolic activity

CD8+ T cells from HIV-1 negative donors or PLWH on ART at different times since treatment initiation were isolated as previously described and cultured for 2 h in the presence of IL-2 (10 IU/ml). Subsequently, 3×10^5 cells from each donor were plated per replicate in DMED media adjusted to a pH of 7.4 in a p96 well plate (Seahorse XFe96 FluxPak Agilent Technologies 102416-100) in the presence of 1 mM Sodium pyruvate, 25 mM Glucose and 1 mM Glutamine. Cells were left unstimulated or activated using Immunocult human CD3/CD28 T Cell Activator (Stem Cell Technologies) for 27 min; and 1 μM oligomycin, 1.5 μM CCCP, and 1 μM Rotenone plus 1 μM Antimycin A were sequentially injected following the Seahorse XF96 Analyzer protocol specifications. Oxygen consumption rate (OCR) and extracellular acidification rate (ECAR) was measured using XF96 Extracellular Flux Analyzers (Seahorse); three measures (5 min) were obtained for each condition. Mitochondrial mass was evaluated as a control by flow cytometry using the MitoTracker Green staining probe (Invitrogen) at a concentration of 6.25 nM per million of cells. In some

experiments, incorporation of glucose was determined by flow cytometry analysis using 2-NBDG (Invitrogen) fluorescent probe.

Statistical analysis

Statistical significance of differences between cells from different or within the same patient cohort under different treatments were assessed using Mann Whitney U or Wilcoxon matched-pairs signed-rank tests. Multiple comparison correction using a Kruskal-Wallis test with post-hoc Dunn's test correction method was applied when appropriate. Chi-square with Yate's correction was used to compare differences in proportions of some parameters within different cell/subject populations. Non-parametric Spearman correlations were performed to test both individual correlations and to generate a correlation network. Association of individual phenotypical and functional data with clinical parameters (years under ART, age at sample collection (y), sex, NADIR $CD4^+$ T cell counts, current $CD4^+$ T cell counts, current $CD8^+$ T cell counts, months from HIV-1 detection to ART initiation) was evaluated using a multiple linear regression model based on a backward elimination technique. Potential confounding variables were gradually removed from the model when they did not modify the β-standardised coefficient of years under ART in more than 10% after their removal. In order to check if the model fulfilled the assumptions for multiple linear regression, several previous analyses were performed. First, an analysis of the standardised residuals was carried out to test for normality, linearity and homogeneity of variances. The dependent variable was transformed to a logarithmic scale in cases it did not follow a normal distribution. To check the absence of autocorrelation, Durbin-Watson index was employed. Finally, the presence of collinearity was evaluated by means of the Tolerance, Variance Inflation Factor (VIF) and Condition Index. Bivariate statistical analyses were performed using GraphPad Prism 7.0 software and multivariate analysis with IBM SPSS Statistics v20.

Role of funders

Funding sources were not involved in any decision regarding this manuscript; including study design, data collection, data analyses, interpretation, or writing of the manuscript.

Results

ART duration determines basal and DC-induced magnitude and polyfunctionality of HIV-specific $CD8^+$ T cell in PLWH

We recruited for our study a cohort of n=49 PLWH who had been under ART for at least 1 year and were characterized by undetectable HIV-1 plasma viremia in blood (Table 1, Figure 1). We evaluated associations between ART duration and detection of HIV-1-specific $CD8^+$ T cells from n=35 individuals in response to autologous monocyte derived dendritic cells (MDDCs) loaded with HIV-1 Gag peptides *in vitro* (Figure 1, Supplementary Figure 1a). As shown in Figure 2a, we observed a significant positive correlation (p=0.0239) between the proportions of IFNγ^+ $CD8^+$ T cells induced in the presence of MDDC loaded with Gag peptides and the number of years on ART. This association was further confirmed using a multivariate model (Table 3). A ROC curve analysis predicted 10.5 years of ART as a cut-off point classifying two PLWH subgroups with different intrinsic optimal induction of HIV-1 specific $CD8^+$T cells (defined as a minimum of 2.5 fold-change in IFNγ expression from baseline) in response to MDDC (Figure 2b). Therefore, we defined two PLWH subgroups of individuals who had been under either long-term ART, for more than a decade (from hereafter, LT-ARTp), or short-term ART, for less than 10 years (from hereafter, ST-ARTp). These two groups were defined by intrinsic differences in age and in NADIR $CD4^+$ T cell counts (p<0.0001 age; p=0.0039 NADIR; Table 1). Consistently, we observed significant differences (p=0.0006) in proportions of IFNγ^+ $CD8^+$ T cells exposed to MDDC loaded with Gag peptides in these two PLWH subgroups (Figure 2b, pie charts). Next, we further assessed whether MDDC primed with 2'3'-c'diAM(PS)2 agonist for Stimulator of Interferon genes (STING) and the Toll like receptor 3 (TLR3) ligand Poly I:C adjuvants and loaded with HIV-1 Gag peptides could potentiate the magnitude and polyfunctionality of autologous HIV-1-specific $CD8^+$ T cells responses in these two separate PLWH subgroups (Supplementary Figure 1a,c). First, we confirmed that MDDCs from each PLWH subgroup were able to similarly and significantly increase CD40 expression after exposure to adjuvants, despite a tendency to higher basal levels on ST-ARTp (Supplementary Figure 1b). In terms of magnitude, co-culture with Gag adjuvant-primed MDDCs significantly increased proportions of INFγ^+ $CD8^+$ T cells from baseline in both ST-ARTp (p=0.0049) and LT-ARTp (p=0.0001) (Figure 2c).

Importantly, Gag-loaded adjuvant-primed MDDCs also significantly increased the frequencies of polyfunctional IFNγ^+ $CD107a^+$ $CD8^+$ T cells in both ST-ARTp (p=0.0012) and LT-ARTp (p=0.0017) compared to baseline (Figure 2d). No association between ART duration and polyfunctionality of HIV-1-specific T cell detection after DC treatment was observed using a multivariate model (Supplementary Table 3). Together, our results indicate that prolonged ART restores intrinsic abilities of HIV-1-specific $CD8^+$ T cells to respond to DC treatment, while adjuvant stimulation enhances polyfunctionality of activated T cells.

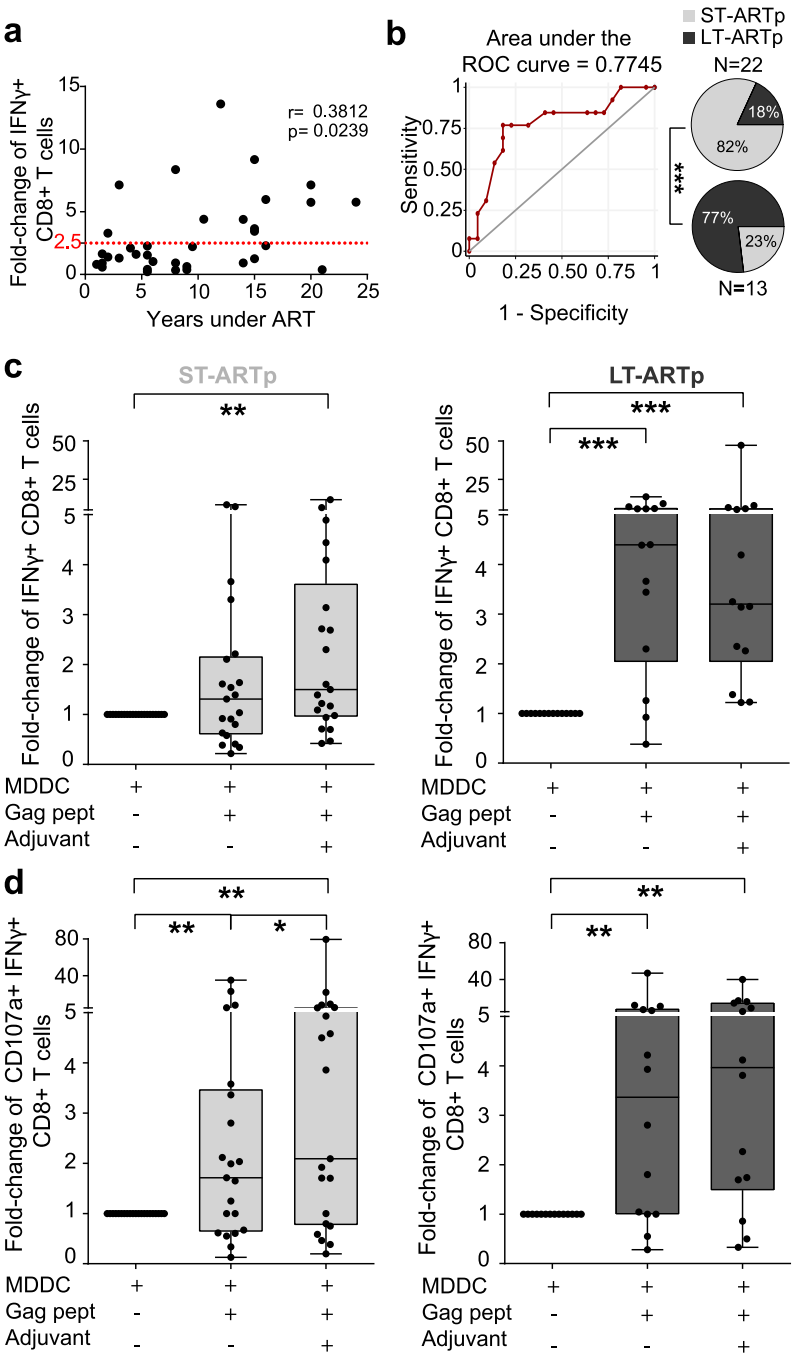

Figure 2. Magnitude and polyfunctionality of HIV-specific CD8$^+$ T cell responses in PLWH on ART. N=35 PLWH (a) Spearman correlation of fold-change in IFNγ expression from total live CD8$^+$ T cells after Gag-peptide presentation by MDDCs, highlighting optimal response established as a minimum of 2.5 fold-change in IFNγ from baseline. Spearman r and p values are shown on the left for each correlation. (b) Left panel showing ROC curve for classification of our cohort based on CD8$^+$ T cell IFNγ response to Gag-loaded MDDC and years under treatment of each individual; and right panel showing pie-charts of the stratification of PLWH based on less than 10 years (ST-ARTp, light grey), or equal or more than 10 years (LT-ARTp, dark grey) of ART duration. ROC curve was calculated with SPSS v20 and statistical significances of pie charts was calculated using a Chi-square test with Yates' correction (***p<0.001). (c-d) Fold-change in IFNγ expression (c) and fold-change in polyfunctional responses (CD107a$^+$ IFNγ^+ cells) (d) from total live CD8$^+$ T cells after stimulation of MDDCs in ST-ARTp (left plots, in light grey) and LT-ARTp (right plots, in dark gray). Statistical significance was calculated using two-tailed Wilcoxon test (*p<0.05; **p<0.01; ***p<0.001; ****p<0.0001).

Coefficients[a]

Model		Standardized Coefficients	Sig.	95% Confidence Interval for B	
				Lower Bound	Upper Bound
	(Constant)		.773	-3.016	2.267
	YEARS_UNDER_ART	.554	.060	-.004	.202
	AGE (y)	.030	.908	-.046	.051
	SEX	-.143	.443	-1.712	.772
	CD4 NADIR	.557	.029	.000	.005
	CUR_CD4	-.253	.253	-.003	.001
	CUR_CD8	.170	.387	.000	.001
	DTC_ART(m)	-.196	.277	-.014	.004
	Dependent Variable: log_fcmddcgag				
	Final model				

Coefficients[a]

Model		Standardized Coefficients	Sig.	95% Confidence Interval for B	
				Lower Bound	Upper Bound
1	(Constant)		.107	-2.215	.226
	YEARS_UNDER_ART	.535	.008	.027	.164
	CD4 NADIR	.383	.051	.000	.004

ANOVA[a]

Model	F	Sig.
Regression	4.193	,024[b]
a. Dependent Variable: log_fcmddcgag		
b. Predictors: (Constant), CD4 NADIR, YEARS_UNDER_ART		

Model Summary[b]

Model	R Square	Adjusted R Square
1	.213	.162
a. Predictors: (Constant), CD4 NADIR, YEARS_UNDER_ART		
b. Dependent Variable: log_fcmddcgag		

***Table 3*: Multiple linear regression model for Fold-change on IFNγ$^+$ CD8$^+$ T cells after priming with Gag-loaded MDDC Initial model.**
log_fcmddcgag=logarithm of Fold-change on IFNγ^+ CD8$^+$ T cells after priming with Gag-loaded MDDC; YEARS_UNDER_ART=years under antiretroviral treatment; AGE (y)=age at sample collection (years); NADIR_CD4=NADIR CD4$^+$ T cell count; CUR_CD4=current CD4$^+$ T cell count; CUR_CD8=current CD8$^+$ T cell count; DTC_ART (m)=months from HIV-1 detection to ART initiation.

Differential restoration of cytotoxic function after DC treatment in CD8$^+$ T cells from LT-ARTp and ST-ARTp

Next, we assessed whether changes on the magnitude and polyfunctionality of HIV-1 Gag-specific CD8$^+$ T cell response after treatment with adjuvant-matured Gag-loaded MDDCs correlated with an increase in their cytotoxic capacity to eliminate HIV-1-infected CD4$^+$ T cells (Figure 1). To address this, CD8$^+$ T cells from ST-ARTp and LT-ARTp pre-stimulated with MDDCs primed in the absence or the presence of Gag peptides and adjuvants were subsequently co-cultured in bulk with autologous CD4$^+$ T cells treated with Raltegavir and Romidepsin (Supplementary Figure 1a). After 24 h, frequencies of cells expressing intracellular HIV-1 p24 were evaluated by FACS (Supplementary Figure 1a,d). As shown in Supplementary Figure 2a, basal detection of HIV-1 p24$^+$ CD4$^+$ T cells cultured with Raltegavir tended to be higher in ST-ARTp compared to LT-ARTp (p=0.0575). Romidepsin treatment increased the frequencies of p24$^+$ cells in 48% of PLWH, and more significantly in LT-ARTp (p=0.042; 53% Supplementary Figure 2b).

Notably, Gag-adjuvant-primed MDDCs enhanced cytotoxic capacities of CD8$^+$ T cells to reduce frequencies of HIV-1 p24$^+$ CD4$^+$ T cells below baseline levels (p<0.0001) in a significantly higher proportion of LT-ARTp individuals compared to ST-ARTp (p=0.0062) (Figure 3a-b, in blue). Restoration of CD8$^+$ T cell function in these PLWH tended to associate with higher levels of polyfunctional HIV-1-specific CD8$^+$ T cells after adjuvant-primed Gag-MDDC (p=0.0294; Figure 3c, lower panel). In contrast, dysfunctional CD8$^+$ T cells unable to reduce proportions of HIV-1 p24$^+$ CD4$^+$ T cells after receiving MDDC stimulation (p=0.0002) were more represented among ST-ARTp compared to the LT-ARTp group (p=0.0062) (Figure 3a-b). We also observed a significant inverse association between the increase of polyfunctional HIV-1-specific CD8$^+$ T responses after MDDC treatment and p24+ cell detection in this PLWH group (p=0.0042; Figure 3c, upper panel). While no significant differences in proportions of p24$^+$ CD4$^+$ T cells induced by Romidepsin were observed between LT-ARTp and ST-ARTp (Supplementary Figure 2c), basal viral reactivation in patients exhibiting dysfunctional CD8$^+$ T cells was

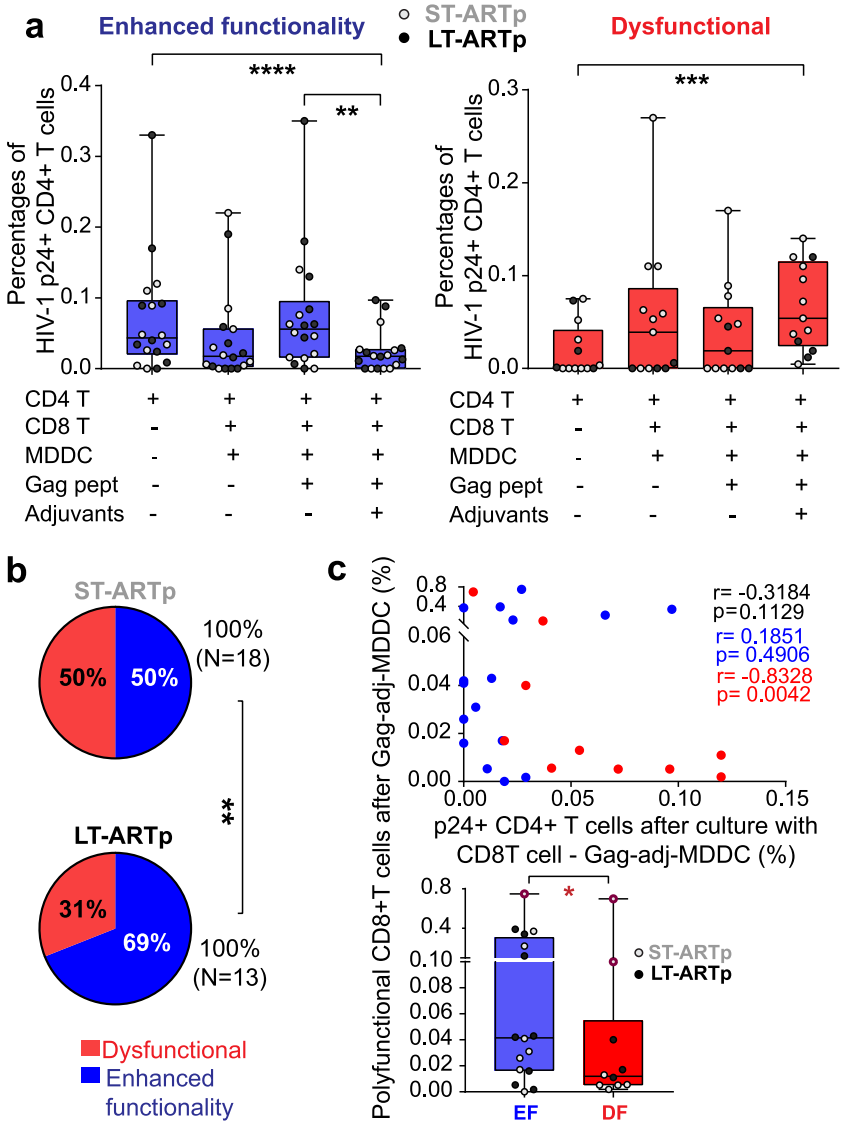

Figure 3. Cytotoxic function of CD8$^+$ T cells from PLWH after DC-treatment. N=31 (N=18 ST-ARTp; N=13 LT-ARTp). (a) Proportions of intracellular HIV-1 p24$^+$ cells from CD4$^+$ T cells cultured in media supplemented with Raltegavir and Romidepsin alone or in the presence of autologous CD8$^+$ T cells and primed with MDDC pre-cultured under the indicated conditions. PLWH were stratified by enhanced (in blue) or dysfunctional (in red) cytotoxic activity of CD8$^+$ T cells eliminating p24$^+$ CD4$^+$ T cell detection after DC treatment. ST-ARTp (light grey) and LT-ARTp (dark grey) PLWH are highlighted within each functional profile. Statistical significance was calculated using two-tailed Wilcoxon test (*p<0.05; **p<0.01; ****p<0.0001). (b) Pie-charts showing percentage of dysfunctional (red) and enhanced functionality (blue) profiles contained within the ST-ARTp and LT-ARTp subgroups. Statistical significance was calculated using a Chi-square test with Yates' correction (**p<0.01). (c) Spearman correlation of proportions of IFNγ^+ CD107a$^+$ (polyfunctional) CD8$^+$ T cells after priming with adjuvant-activated Gag-loaded MDDC *vs* p24$^+$ T cells present in co-culture with these CD8$^+$ T cells activated with adjuvant-primed Gag-loaded MDDC (N=14 enhanced functionality, and N=12 dysfunctional; Upper panel). P and r values are shown on the right, in black for total values, in red for dysfunctional, and in blue for enhanced functionality. Proportions of IFNγ^+ CD107a$^+$ (polyfunctional) CD8$^+$ T cells after priming with adjuvant-activated Gag-loaded MDDC comparing enhanced functionality (EF) and dysfunctional (DF). Statistical significance was calculated using two-tailed Mann-Whitney U test after outlier removal using the ROUT method (*p<0.05).

significantly lower (p=0.0087; Supplementary Figure 2d) and tended to be induced in the presence of unstimulated MDDC and CD8$^+$ T cells (Figure 3a). We also observed that proportions of IFNγ^+ CD8$^+$ T cells were higher in ST-ARTp in response to MDDC in the absence of HIV-1 Gag peptides (p=0.0317), and a similar non-significant trend was present in PLWH exhibiting dysfunctional CD8$^+$ T cells (Supplementary Figure 3a-c).

Therefore, functional restoration of HIV-1-specific CD8$^+$ T cells from PLWH in response to Gag-adjuvant-primed MDDCs might be influenced by multiple parameters including their basal state, the increase in polyfunctionality after DC stimulation, the basal reactivation of p24$^+$ cells and the number of years on ART.

Differential memory subset distribution and distinct patterns of co-expression of checkpoint inhibitory receptors in CD8$^+$ T cells from ST-ARTp and LT-ARTp

Differences in basal response to HIV-1 Gag-peptide stimulation and functional enhancement of CD8$^+$ T cells from ST-ARTp and LT-ARTp PLWH after treatment with Gag-adjuvant-primed MDDCs could be associated to either deficiency on DC activation, memory subset distribution or immune exhaustion of CD8$^+$ T cells. We previously showed that our adjuvant combination similarly increased the percentage of CD40$^+$ MDDCs in both ST-ARTp and LT-ARTp (Figure 1, Supplementary Figure 1b). Interestingly, lower plasma Tryptophan levels (p=0.0495) and higher expression of IDO-1 (p=0.0221) were present on LT-ARTp compared to ST-ARTp, suggesting that dysfunctional CD8$^+$ T cells in the latter were not due to a tolerogenic environment (Supplementary Figure 4a).

Since dysfunction of HIV-1-specific CD8$^+$ T cell responses has been linked to reduced percentages of central memory (CM) cells[32], we next analysed the proportions of different CD8$^+$ T cell memory subsets in ST-ARTp and LT-ARTp (Figure 1). We observed that CD8$^+$ T cells from LT-ARTp contained higher proportions of CCR7$^+$ CD45RO$^+$ CM cells than in ST-ARTp (p=0.0362), reaching similar percentages to HIV-1 negative controls (HC; Figure 4a). On the contrary, CD8$^+$ T cells from ST-ARTp tended to present higher proportions of CCR7- CD45RO+ effector memory (EM) and CCR7$^-$ CD45RO$^-$ terminally differentiated (TD) cells (Figure 4a). Preservation of CM cells was most evident in LT-ARTp that had received treatment shortly after diagnosis (p=0.0239; Figure 4a, right plot).

We next asked whether differences on proportions of CD8$^+$ T cell memory subsets from LT-ARTp and ST-ARTp could also be associated with the immune exhaustion state of these lymphocytes (Figure 1). In addition to inducing maturation, adjuvant treatment also tends to increase expression of ligands for immunomodulatory checkpoint inhibitory receptors such as PD-L1, CD155 and Galectin-9 on MDDCs (Supplementary Figure 4b), suggesting that binding of these receptors might limit the functional improvement of CD8$^+$ T cells from PLWH after MDDC stimulation. In addition, the co-expression of checkpoint inhibitory receptors has been previously associated to terminal exhaustion on T cells.[20,22,40] Therefore, we determined the surface co-expression of PD1, TIGIT and TIM3 in memory CD8$^+$ T cells from ST-ARTp, LT-ARTp and HC by flow cytometry (Supplementary Figs. 5a-b). Notably, CD8$^+$ T cells from ST-ARTp were significantly enriched on PD1$^+$ TIGIT$^+$ TIM3$^-$ CM and EM cells in contrast to LT-ARTp, whose CD8$^+$ T cells contained significantly higher proportions of the PD1$^-$ TIGIT$^+$ TIM3$^-$ simple positive memory (CM, p=0.0049; EM, p=0.0061) cells, similarly to HC (Figure 4 b-c, Supplementary Figure 5a-b). CD8$^+$ T cells from ST-ARTp also contained higher proportions of PD1$^+$TIM3$^+$ within the TIM3$^+$ CM and EM populations compared to LT-ARTp, which were more enriched in PD1$^-$TIM3$^+$ cells (CM, p=0.001; EM, p=0.0059; Figure 4d-e, Supplementary Figure 5a-b). In addition, PD1$^+$ TIGIT$^+$ TIM3$^+$ cells were infrequent but their proportions were significantly higher in EM CD8$^+$ T cells from ST-ARTp, compared with LT-ARTp (p=0.0339) and HC (p=0.0506) (Supplementary Figure 5b). Notably, proliferating CM and EM CD8$^+$ T cells stimulated with allogeneic adjuvant-primed MDDCs selectively induced TIM3 expression, whereas the induction of TIGIT and PD1 expression was weaker and not restricted to proliferating cells (Supplementary Figure 6a-c). Therefore, non-overlapping co-expression profiles of different checkpoint inhibitory receptors induced after MDDC treatment are present on CD8$^+$ T cells from PLWH at different times since ART initiation.

Differential induction of glycolytic metabolic activity in CD8$^+$ T cells from PLWH subgroups

Metabolic plasticity and glycolytic activity have been associated with exhaustion, effector function of CD8$^+$ T cells and with their ability to mediate viral control.[32,41] Thus, we focused on studying the metabolic profiles of CD8$^+$ T cells from LT-ARTp and ST-ARTp with either high cytotoxic function or dysfunctional characteristic and displaying opposite co-expression profiles of checkpoint receptors. These patients were also matched by age and sex with cells from HIV negative donors (Tables 1 and 2). Then, we studied mitochondrial respiration and the glycolytic rate by determining oxygen consumption (OCR) and extracellular acidification rate (ECAR) on CD8$^+$ T cells from these PLWH groups and HC at baseline and after TCR/CD28 stimulation (Figure 1, Figure 5a-b, Supplementary Figure 7a-b, also see Methods). While CD8$^+$ T cells from HC induced significantly higher OCR after TCR stimulation (p=0.0222 at 83min), OCR values were significantly lower on stimulated CD8$^+$ T cells from ST-ARTp compared to HC (p=0.0090 at 83min) and partially preserved in LT-ARTp (Figure 5a, Supplementary Figure 8a,c), suggesting potential defects on mitochondrial respiration on PLWH that were more marked in cells from ST-ARTp. In addition, TCR-stimulated CD8$^+$ T cells from LT-ARTp showed significantly higher ECAR induction compared to HC (p=0.0201, 73min), suggesting increased ability to induce glycolysis (Figure 5b, Supplementary Figure 8b,d). CD8$^+$ T cells from ST-ARTp were

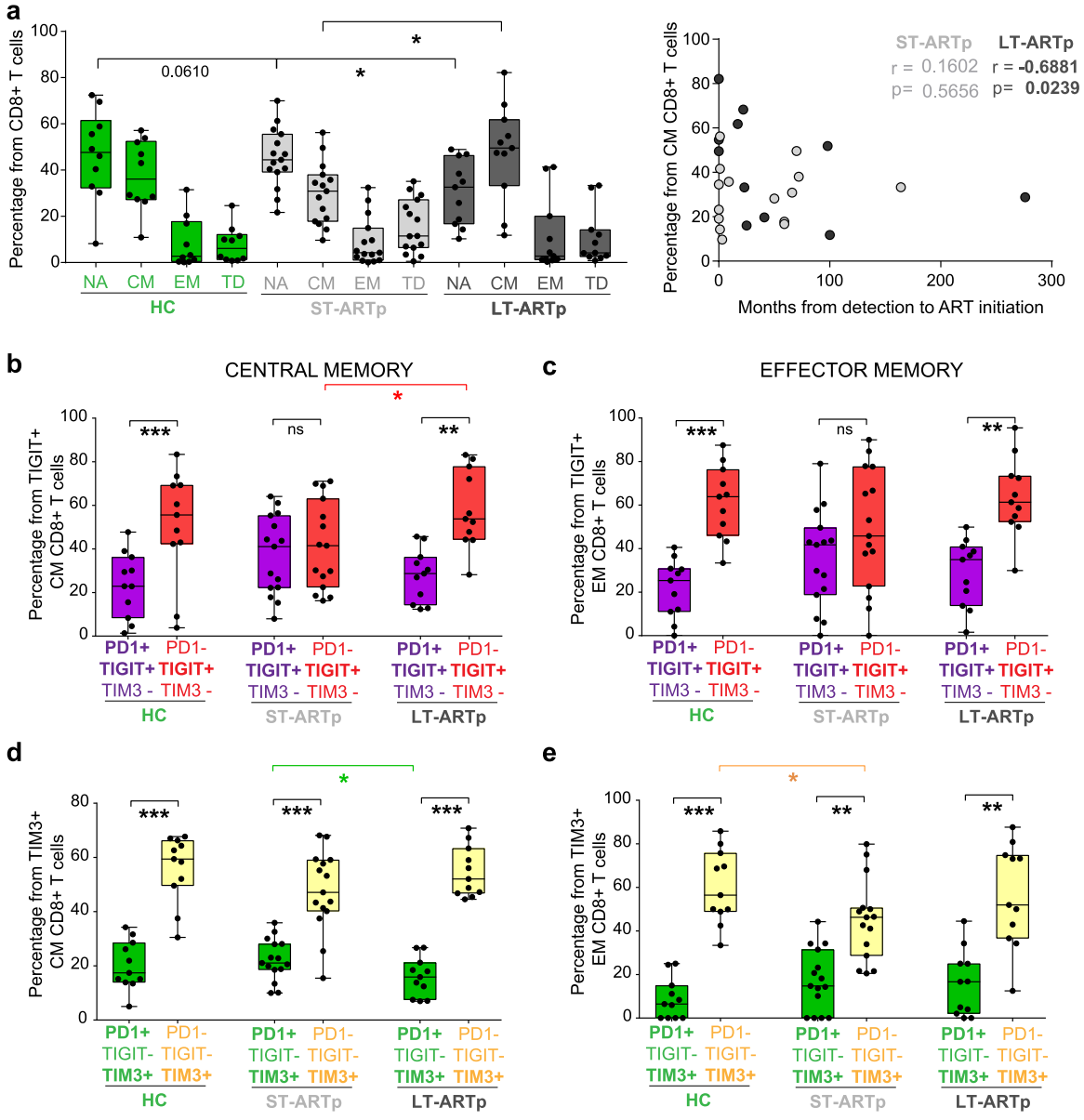

Figure 4. Memory subset distribution and co-expression of checkpoint inhibitor receptors in CD8$^+$ T cells from different PLWH subgroups. N=11 HIV-1 negative controls (HC); N=15 ST-ARTp; N=11 LT-ARTp. (a) Percentage of naïve, NA (CCR7$^+$ CD45Ro$^-$); central memory, CM (CCR7$^+$ CD45Ro$^+$); effector memory, EM (CCR7$^-$ CD45Ro$^+$); and terminally differentiated, TD (CCR7$^-$ CD45Ro$^-$) CD8$^+$ T cells from HIV negative controls (HC; green bars), ST-ARTp (light grey bars) and LT-ARTp (dark grey bars). Statistical significance was calculated using two-tailed Mann-Whitney U test (*p<0.05). On the right, Spearman correlations between the percentage of CM CD8$^+$ T cells and months since HIV-1 infection diagnosis to ART initiation for ST-ARTp (light grey) and LT-ARTp (dark grey dots). Spearman r and p values are shown on the left for each correlation. (b-e) Proportion of PD1$^+$TIGIT$^+$TIM3$^-$ (b-c; purple) or PD1$^+$TIGIT$^-$TIM3$^+$ (d-e; green) populations from total TIGIT$^+$ or TIM3$^+$ cells, compared to PD1$^-$TIGIT$^+$TIM3$^-$ (B-C; red) or PD1-TIGIT$^-$TIM3$^+$ (D-E; yellow) population from total TIGIT$^+$ or TIM3$^+$ populations. Statistical significance between the mentioned double and single positive populations was calculated using two-tailed matched pairs Wilcoxon test (**p<0.01; ***p<0.001) within each participant group and using two-tailed Mann-Whitney U test (*p<0.05) between different individuals.

less efficient inducing ECAR after TCR stimulation and not significantly different from HC (Figure 5b, Supplementary Figure 8b,d). The observed changes were not due to differences in glucose uptake or total mitochondrial mass between ST-ARTp, LT-ARTp and HC subgroups (Supplementary Figure 8e-f). Alternatively, basal transcriptional levels of the glucose metabolism regulator HIF1α were increased on memory CD8$^+$

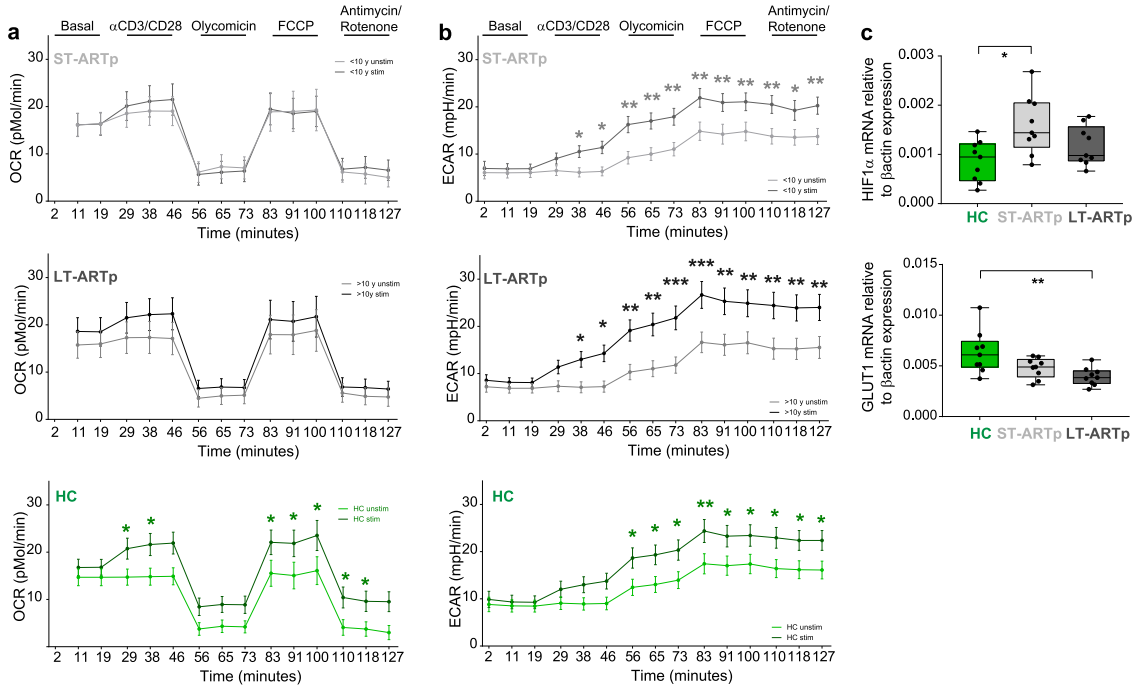

Figure 5. CD8$^+$ T cell oxidative and glycolytic metabolism in PLWH. (a-b) Oxygen consumption rate (a; OCR) and extracellular acidification rate (b; ECAR) in CD8$^+$ T cells from PLWH comparing basal (light line) and TCR activated (dark line) cells from ST-ARTp (N=10; upper plots; light grey), LT-ARTp (N=10; middle plots; dark grey), and HIV-1 negative controls (HC; N=12; lower plots; green). Statistical significance per each timepoint was calculated with a multiple t test analysis. (c) RT-qPCR analysis of HIF1α (upper) and GLUT1 (lower) transcriptional expression normalized to β–actin mRNA levels in memory CD45RA$^-$ CD8$^+$ T cells isolated from total PBMCs from HIV negative controls (HC; N=9; green) and PLWH (ST-ARTp; N=9; light grey, and LT-ARTp; N=9; dark grey). Statistical significance between double and single positive populations was calculated using two-tailed Wilcoxon test (*p<0.05).

T cells from ST-ARTp compared to HC (p=0.0106). Similar patterns of expression were observed for other glycolysis regulators such as PGK1 and GAPDH on ST-ARTp (Supplementary Figure 9a). In addition, mRNA levels of GLUT1 in memory CD8$^+$ T cells from LT-ARTp were significantly lower compared to HC (p=0.0056; Figure 5c). Together, our results indicate that prolonged ART might preserve the ability to induce glycolysis and mitochondrial respiration after TCR stimulation in CD8$^+$ T cells from PLWH.

Combined blockade of checkpoint inhibitory receptors and administration of glycolysis promoting drugs efficiently restores cytotoxic function of CD8$^+$ T cell from ST-ARTp

Specific combinations of PD1, TIGIT and TIM3 checkpoint inhibitory receptors may differentially affect the glucose metabolism[26-28] and function of CD8$^+$ T cells from ST-ARTp and LT-ARTp (Figure 1). Supporting this possibility, we observed significant positive correlations between the increase on maximal glycolytic profiles after TCR activation on CD8$^+$ T cells, and the percentages of single positive TIGIT (p=0.0094 CM; p=0.0872 EM) or TIM3 (p=0.0161 CM; p=0.0037 EM) cells within memory cell subsets (Figure 6a-b, upper panels; Supplementary Figure 9b). Opposite associations were observed between higher ratios of co-expression of PD1 and TIGIT (p=0.0401 CM; p=0.0623 EM) or TIM3 (p=0.0567 CM; p=0.0503 EM) and the induction of glycolysis in these memory CD8$^+$ T cell subsets (Figure 6a-b, lower panels; Supplementary Figure 9b). Age also correlated with higher increase in ECAR (p=0.077), lower PD1 and TIGIT co-expression (p=0.058 CM, p=0.072 EM) and higher proportions of TIM3$^+$ PD-1$^-$ cells (p=0.105 CM, p=0.013 EM) (Supplementary Figure 9b). Therefore, our data demonstrate that TIGIT and PD1 co-expression in CM and EM CD8$^+$ T cells correlate with impaired ability to induce glycolysis in total CD8$^+$ T cells from PLWH.

Finally, we asked whether simultaneous blockade of multiple checkpoint inhibitory receptors and/or treatment with pro-glycolytic drugs such as Metformin might more efficiently restore functional properties of CD8$^+$ T cells from ST-ARTp after DC-treatment (Figure 1). To test these strategies, we stimulated dysfunctional CD8$^+$ T cells from ST-ARTp with autologous adjuvant-primed and Gag-peptide loaded MDDCs in the presence of individual or a cocktail of antibodies specific for PD1, TIGIT and TIM3 alone or in

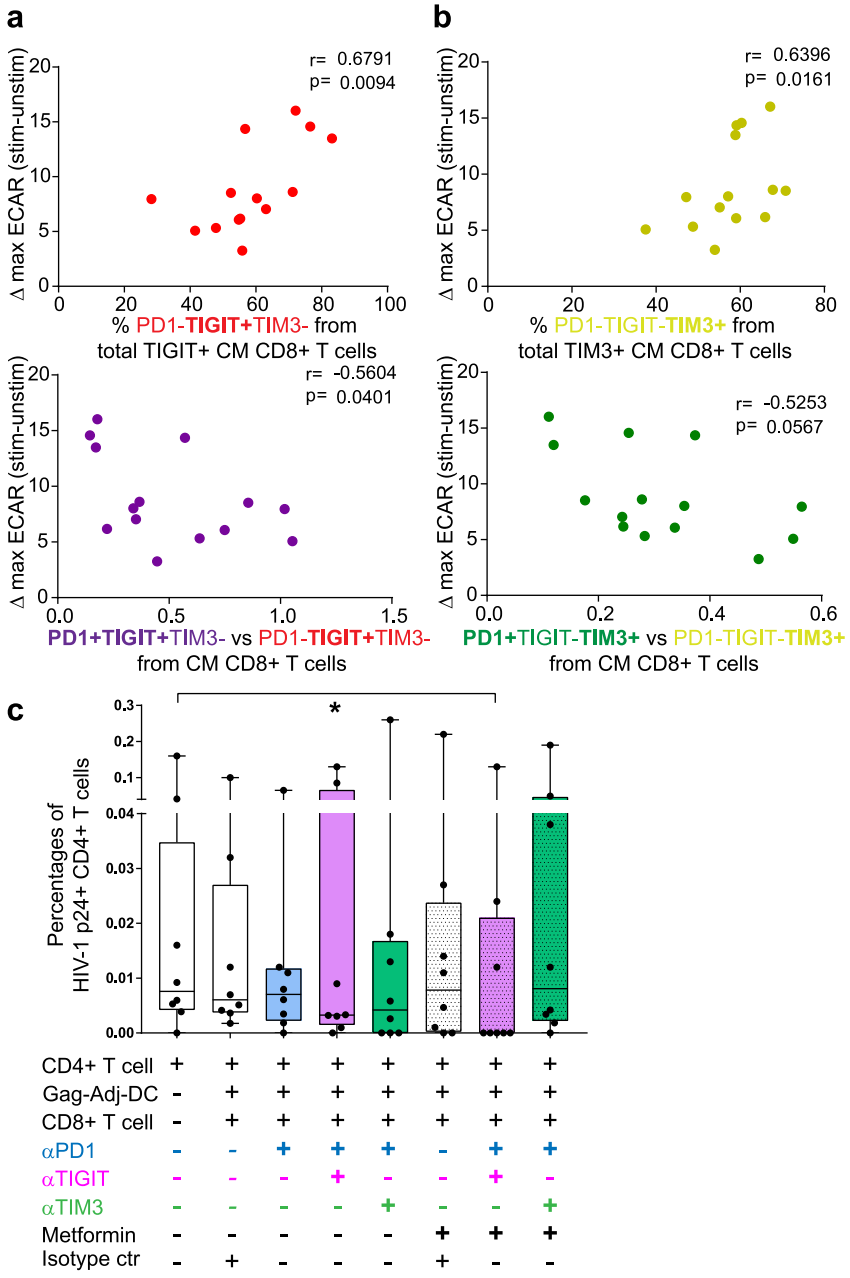

Fig. 6. Correlation and fine-tuning of glycolytic metabolism and memory exhaustion in CD8$^+$ T cell from PLWH. (a-b) Spearman correlations between ΔECAR at maximal activation after TCR stimulation (73 minutes) and proportions of PD1$^-$TIGIT$^+$TIM3$^-$ (a, upper panel; N=14; red) or PD1-TIGIT$^-$TIM3$^+$ (b, upper panel; N=14; yellow) to total TIGIT$^+$ or TIM3$^+$ cells or ratios of the indicated populations (lower plots; PD1 *vs* TIGIT purple and red; PD1 *vs* TIM3 green and yellow; N=14 each) within central memory CD8$^+$ T cells. Spearman r and p values are shown on the upper left area of each plot. (c) Proportions of p24$^+$ cells from total live CD4$^+$ T cells to basal CD4$^+$ T cells p24$^+$ detection to the different MDDC and CD8$^+$ T cell treated conditions (N=8). Light purple bars indicate the use of anti-PD1 and anti-TIGIT blocking antibodies in combination; light green bars indicate the use of anti-PD1 and anti-TIM3 blocking antibodies combination. Stripped bars indicate the use of 5 mM Metformin, either alone or in combination with the blocking antibodies. Statistical significance to the CD4$^+$ T cell basal condition was calculated using two-tailed Wilcoxon test (*p<0.05).

combination with Metformin at a concentration capable of inducing ECAR without affecting viability (Supplemental Figure 9c). As shown in Figure 6c, the combined treatment of Metformin with anti-TIGIT and anti-PD1 mAbs was more efficient in restoring the cytotoxic capacities of CD8$^+$ T cells from ST-ARTp and

significantly reduced proportions of $p24^+$ cells compared to $CD4^+$ T cells alone (p=0.0156), in contrast to other combinations or corresponding isotype controls. Together, our data indicate that simultaneous blockade of TIGIT and PD1 combined with pro-glycolytic metabolism drugs can improve the functionality of HIV-1-specific $CD8^+$ T cells from ST-ARTp after MDDC stimulation.

Discussion

The present study evaluated the efficacy of adjuvant-primed MDDC as a potential therapeutic candidate to restore cytotoxic capacities of $CD8^+$ T cell from different groups of PLWH, who are under ART and characterized by undetectable plasma HIV-1 viral load. Previous studies have suggested that innate-specific adjuvant-mediated activation could be useful to potentiate HIV-1-specific $CD8^+$ T cells.[42,43] However, such systemic adjuvant administration approaches failed in preventing viral rebound after ART interruption.[44-49] Our therapeutic approach based on the activation of DCs has been previously associated with increased polyfunctional HIV-1-specific $CD8^+$ T cell responses in lymphoid tissues *in vivo*.[17] Thus, our immunotherapy strategy allows avoiding bystander activation of cells other than DCs in response to adjuvants. We have also shown that this method can also be useful to induce polyfunctional HIV-1-specific $CD8^+$ T cell responses from PLWH resulting in reduction of HIV-infected $CD4^+$ T cells *in vitro*.

We have also demonstrated that the years under ART determine the basal capacity of HIV-1 specific $CD8^+$ T cells to respond to MDDC stimulation and antigen presentation. We have observed differences on checkpoint inhibitory receptor phenotypes and on frequencies of central and effector memory $CD8^+$ T cells that are associated with the time since ART initiation. These results are in line with previous studies reporting the recovery from immune exhaustion upon HIV-1 pharmacological suppression, as well as differences in metabolism in these treated individuals.[32,50-52] Our study identifies immunological and metabolic patterns that are specifically associated with effective responses of $CD8^+$T cells to DC-based treatment in different subgroups of PLWH. Our data might be useful to personalize immunotherapies in different groups of PLWH to more efficiently mimic $CD8^+$ T cell responses observed in spontaneous HIV-1 controllers[53,54] or to increase the frequencies of suppressed individuals capable of controlling viral replication after treatment interruption.[13,55-58]

We have defined that prolonged treatment duration is required to restore phenotypical and effector capacities of $CD8^+$ T cells and to respond to MDDC-based HIV-1 vaccines. Those results are in line with previous studies by Perdomo-Celis *et al*[59], demonstrating that $CD8^+$ T cell cytotoxic and polyfunctional capacities are reduced in PLWH compared to HIV-1 negative individuals, and that ART only slightly reinvigorates the cytotoxic capacities after two years of treatment. We have found a negative correlation between the time from HIV diagnosis to ART initiation and preserved proportions of CM $CD8^+$ T cell subpopulation in LT-ARTp. These findings are in agreement with previous studies suggesting heterogenic efficacy of immunotherapy boosting HIV-1 specific $CD8^+$ T cells and the importance of early ART initiation preserving immune function of memory T cells.[43,60] In addition, previous studies suggest that higher HIV-1 DNA is associated with increased detection of HIV-1 specific T cells[61]; in our study, we have not observed significant differences between basal HIV-1 $p24^+$ levels in ST-ARTp and LT-ARTp PLWH. However, higher basal p24 expression and differential efficacy of Romidepsin mediating effective viral reactivation in the presence of MDDC might be linked to dysfunctional response of $CD8^+$ T cells. In fact, higher induction of $IFN\gamma^+$ $CD8^+$ T cells in the presence of MDDC without Gag peptide stimulation tended to be detected in ST-ARTp PLWH with dysfunctional response to immunotherapy. Therefore, inflammatory responses by DC or bystander cells might also affect antigen availability and functionality of HIV-1-specific cells as previously suggested in HIV-1[62,63] and HBV infections.[64]

Limitations of the present study include the low sample size from our PLWH and HIV negative cohorts matched by age and sex and the unavailability to include all participants in every individual analysis performed, and finally considering $IFN\gamma$ and CD107a co-expression as a readout of polyfunctional HIV-1-specific T cells without taking into account their co-expression with $TNF\alpha$, which has been associated with durable and efficient $CD8^+$ T cell responses.[17,65] In addition, age was intrinsically higher in the LT-ARTp cohort due to prolonged treatment duration, leading to significant associations of multiple functional and phenotypical data with this parameter. Therefore, additional studies using a larger number of patients with similar demographic characteristics and analysing TCR specificity by tetramer staining should be conducted.

On the other hand, our study provides relevant information about the parameters determining the exhaustion and metabolic state of $CD8^+$ T cells and their connection with the response to DC immunotherapy. We have described that ST-ARTp contain lower proportions of CM $CD8^+$ T cells and that those cells are characterized by higher co-expression of TIGIT and PD1. Interestingly, LT-ARTp displayed higher percentages of CM $CD8^+$ T cells, which were more enriched by single expression of TIGIT or TIM3. While previous studies had described that co-expression of checkpoint inhibitory receptors might be associated with reduced cytotoxic activity of HIV-1-specific $CD8^+$ T cells in PLWH[40,66-68], our study provides new information suggesting that different combinations of specific checkpoint inhibitory receptors might differentially affect

functional exhaustion of T cells. The role of PD1 limiting the development and effector function of memory $CD8^+$ T cells, and the beneficial effect of PD1 blockade have already been described in cancer and also in other viral infections. Anti-PD1 mAb based therapies have yielded promising results in animal models of SIV-infection in macaques, enhancing specific $CD8^+$ T cell responses and reducing the plasma viral load, resulting in enhanced survival of the animals. However, they were not sufficient to prevent viral rebound after treatment interruption.[13,55,56] Thus, modulation of additional checkpoint inhibitory receptors and metabolic pathways might be required to more efficiently reinvigorate functional HIV-specific $CD8^+$ T cells in PLWH. In this regard, we have demonstrated that the combined blockade of anti-PD1 and anti-TIGIT improves the cytotoxic capacities of $CD8^+$ T cells from ST-ARTp against HIV-infected $CD4^+$ T cells more effectively than anti-PD1 blockade alone. These data are supported by similar results in a gastric cancer animal model.[27] Our results also indicate that combined TIM3 and PD-1 blockade seemed to disrupt cytotoxic function of $CD8^+$ T cell from ST-ARTp individuals. Although TIM3 blockade inhibited T regulatory function and has yielded promising results on different cancer model, TIM3 has also been reported as a marker of proliferating $IFN\gamma^+$ Th1 cells, key in the antiviral response. Thus, the effector function of these cells could be dependent on TIM3 expression.[69,70] In this regard, $CD8^+$ T cells co-expressing PD1 and TIM3 are more prone to respond to PD1 blockade in cancer therapies.[31] Therefore, it is unclear whether TIM3 expression might be beneficial or detrimental for $CD8^+$ T cell response generation in PLWH and different combinations with other checkpoint receptors should be further studied. In addition, myeloid cells from LT-ARTp are characterized by higher IDO-1 expression and lower plasma Tryptophan detection than ST-ARTp. IDO-1 is induced upon HIV-1 infection and its expression is reduced after ART initiation[71,72], but long-term treatment or age might also affect the expression or function of this molecule.[73,74] Despite these results, DC-therapy more efficiently restores HIV-1 specific $CD8^+$ T cells in LT-ARTp. Thus, the impact of IDO-1 facilitating durable functional HIV-1 specific T cells should be investigated.

Another key aspect of our study is the fact that we have analysed the association between phenotypical and functional differences on $CD8^+$ T cells from PLWH exposed to DC with checkpoint inhibitory markers expression and other processes associated to exhaustion, such as mitochondrial respiration and the glucose metabolism. Previous studies have reported a correlation between glycolysis increase and effective cytotoxic functions of $CD8^+$ T cells against HIV-infected cells in treated PLWH.[75] Reduced glycolysis has been associated to HIV-1 latency and oxidative stress in infected individuals.[76] We reported higher induction of ECAR after TCR stimulation in $CD8^+$ T cells from LT-ARTp displaying effective cytotoxic function against HIV-1-infected cells, whilst enrichment of $TIGIT^+$ $PD1^+$ in $CD8^+$ T cells from ST-ARTp associated to reduced ability to increase ECAR upon TCR activation. We were able to describe a correlation between $CD8^+$ T cell effector and cytotoxic functions upon MDDC activation, basal $CD8^+$ T cell memory exhaustion phenotypes, metabolic dysfunctional state and years under ART in a cohort of PLWH. However, an important limitation from our study is that we did not directly address the metabolic and functional properties of $CD8^+$ T cells from ST-ARTp and LT-ARTp isolated based on the differential expression of checkpoint receptors. In addition, immunosenescence has been described as a process affecting metabolism throughout adult life to elderly; however, $CD8^+$ T cells from LT-ARTp characterized by older age, still displayed preserved function and metabolic properties similar to our HIV negative cohort. Oxidative metabolism seems to be largely altered in PLWH, however, the mechanisms leading to these observations have not been assessed. The role of T cell factor-1, which is expressed by effective long-lived PD1-low memory $CD8^+$ T cells during chronic infections[31,77], and mitochondrial fission and fusion[78,79] may be also playing a role in these processes, contributing to the differences on the metabolic dysfunction described in this study.

Our PLWH cohort was defined by individuals on ART, with undetectable plasma HIV-1 viral load (<20 mRNA copies/ml), with no co-infection with HCV, and $CD4^+$ T cell counts higher than 400 cells/ml, since prolonged treatment in PLWH has been described to partially restore $CD8^+$ T cell function and reduce exhaustion, compared to non-treated PLWH.[80-82] This allowed us to evaluate the capacity of our adjuvant-DC strategy to induce $CD8^+$ T cell responses in PLWH at different times since treatment initiation. However, some of the observed responses and differences might not be present in viremic PLWH with low $CD4^+$ and $CD8^+$ T cell counts. In these patients, memory $CD8^+$ T cell populations could be more enriched in a terminally and exhausted memory phenotype, and therefore less capable of mediating competent cytotoxic effector responses even after DC stimulation. Therefore, further analysis should address the effectiveness of DC therapy and the proposed combined treatment with blocking antibodies and glycolysis inductors for these particular populations of PLWH reinvigorating their memory T cells. In conclusion, our study identifies specific immunometabolic parameters for different groups of PLWH defined by antiretroviral treatment duration, non-overlapping expression of checkpoint inhibitory receptors and metabolic state of $CD8^+$ T cells that can be modulated through personalized therapies to fine-tune functional HIV-1 $CD8^+$ T cell responses, providing new tools to advance and improve DC-based HIV-1 vaccines.

Contributors

EMG developed the research idea and study concept, designed, supervised the study and verified the underlying data. MCM designed and conducted most experiments of the study. ISC contributed to functional assays. IT, MCM, CDA performed analysis of checkpoint receptors and proliferation in MLR experiments from the study. NMC, MCM and EMG designed and performed Seahorse experiments. MCM, ISC, CDA processed peripheral blood samples from PLWH and HIV negative donors. MJB, HDF, NMC provided critical feedback during experimental design and execution phases of the studies and were directly involved in the experiments and verified the underlying data. MJC provided reagents for transcriptional analysis of metabolic regulators and provided critical feedback. PMF performed the ROC curve and multivariate analyses. FSM, AA, MAMF, IDS, LGF, and JS provided peripheral blood from PLWH and HIV negative controls, reagents, clinical expertise and participated on the analysis of the data. All authors have read and approved the final version of this manuscript.

Data sharing statement

The data that support the findings of this study will be available upon reasonable request to the corresponding author of the study.

Declaration of interests

The authors have declared that no conflict of interest exists.

Acknowledgements

We would like to thank the NIH AIDS Reagent Program, Division of AIDS, NIAID, NIH for providing HIV-1 PTE Gag Peptide Pool from NIAID, DAIDS (cat #11057) for the study. We would also like to thank Álvaro Serrano Navarro, for his help on adapting the linear mixed model previously described by Martin-Cófreces N. et al[83] to our data. Graphical schematic representations were created with BioRender.com.

EMG was supported by the NIH R21 program (R21AI140930), the Ramón y Cajal Program (RYC2018-024374-I), the MINECO/FEDER RETOS program (RTI2018-097485-A-I00), by Comunidad de Madrid Talento Program (2017-T1/BMD-5396) and by Gilead becas de investigación (GLD19/00168). EMG and IDS are supported by Centro de Investigación Biomédica en Red (CIBERINF) de Enfermedades Infecciosas (CB21/13/00107). MCM was supported by NIH R21 program (R21AI140930), "La Caixa Banking Foundation (H20-00218) and Gilead becas de investigación (GLD19/00168). MJB is supported by the Miguel Servet program funded by the Spanish Health Institute Carlos III (CP17/00179), the MINECO/FEDER RETOS program (RTI2018-101082-B-I00), and Fundació La Marató TV3 (201805-10FMTV3). EMG and MJB are both funded by "La Caixa Banking Foundation (H20-00218) and by REDINCOV grant from Fundació La Marató TV3. FSM was supported by SAF2017-82886-R and PDI-2020-120412RB-I00 grants from the Ministerio de Ciencia e Innovación, and HR17-00016 grant from "La Caixa Banking Foundation. HF was funded by PI21/01583 grant from Ministerio de Ciencia e Innovación, Instituto de Salud Carlos III. MJC was supported by PID2019-104406RB-I00 from Ministerio de Ciencia e Innovación. ISC was funded by the CM21/00157 Rio-Hortega grant. IT was supported by grant for the promotion of research studies master-UAM 2021.

Supplementary materials

Supplementary material associated with this article can be found in the online version at doi:10.1016/j.ebiom.2022.104090.

References

1 Pallikkuth S, Sharkey M, Babic DZ, et al. Peripheral T follicular helper cells are the major HIV reservoir within central memory CD4 T cells in peripheral blood from chronically HIV-infected individuals on combination antiretroviral therapy. *J Virol*. 2015;90(6):2718–2728.
2 Henderson LJ, Reoma LB, Kovacs JA, Nath A. Advances toward curing HIV-1 infection in tissue reservoirs. *J Virol*. 2020;94(3).
3 Banga R, Munoz O, Perreau M. HIV persistence in lymph nodes. *Curr Opin HIV AIDS*. 2021;16(4):209–214.
4 Cohn LB, Chomont N, Deeks SG. The biology of the HIV-1 latent reservoir and implications for cure strategies. *Cell Host Microbe*. 2020;27(4):519–530.
5 Mohamed H, Miller V, Jennings SR, Wigdahl B, Krebs FC. The evolution of dendritic cell immunotherapy against HIV-1 infection: improvements and outlook. *J Immunol Res*. 2020;2020:9470102.
6 Deeks SG. HIV: shock and kill. *Nature*. 2012;487(7408):439–440.
7 Shan L, Deng K, Gao H, et al. Transcriptional reprogramming during effector-to-memory transition renders CD4(+) T cells permissive for latent HIV-1 infection. *Immunity*. 2017;47(4):766–775.e3.
8 Martinez-Picado J, Deeks SG. Persistent HIV-1 replication during antiretroviral therapy. *Curr Opin HIV AIDS*. 2016;11(4):417–423.
9 Walker-Sperling VE, Cohen VJ, Tarwater PM, Blankson JN. Reactivation kinetics of HIV-1 and susceptibility of reactivated latently infected CD4+ T cells to HIV-1-specific CD8+ T cells. *J Virol*. 2015;89(18):9631–9638.
10 O'Connell KA, Bailey JR, Blankson JN. Elucidating the elite: mechanisms of control in HIV-1 infection. *Trends Pharmacol Sci*. 2009;30(12):631–637.
11 Pantaleo G, Levy Y. Therapeutic vaccines and immunological intervention in HIV infection: a paradigm change. *Curr Opin HIV AIDS*. 2016;11(6):576–584.
12 Bekerman E, Hesselgesser J, Carr B, et al. PD-1 blockade and TLR7 activation lack therapeutic benefit in chronic simian immunodeficiency virus-infected macaques on antiretroviral therapy. *Antimicrob Agents Chemother*. 2019;63(11).
13 Seddiki N, Lévy Y. Therapeutic HIV-1 vaccine: time for immunomodulation and combinatorial strategies. *Curr Opin HIV AIDS*.. 2018;13(2):119–127.
14 Martin-Gayo E, Buzon MJ, Ouyang Z, et al. Potent cell-intrinsic immune responses in dendritic cells facilitate HIV-1-specific T cell immunity in HIV-1 elite controllers. *PLoS Pathog*. 2015;11(6):e1004930.
15 Martin-Gayo E, Cole MB, Kolb KE, et al. A reproducibility-based computational framework identifies an inducible, enhanced antiviral state in dendritic cells from HIV-1 elite controllers. *Genome Biol*. 2018;19(1):10.

16 Decout A, Katz JD, Venkatraman S, Ablasser A. The cGAS-STING pathway as a therapeutic target in inflammatory diseases. *Nat Rev Immunol*. 2021;21(9):548–569.
17 Calvet-Mirabent M, Claiborne DT, Deruaz M, et al. Poly I:C and STING agonist-primed DC increase lymphoid tissue polyfunctional HIV-1-specific CD8(+) T cells and limit CD4(+) T-cell loss in BLT mice. *Eur J Immunol*. 2021.
18 Kristoff J, Rinaldo CR, Mailliard RB. Role of dendritic cells in exposing latent HIV-1 for the kill. *Viruses*. 2019;12(1).
19 Kristoff J, Palma ML, Garcia-Bates TM, et al. Type 1-programmed dendritic cells drive antigen-specific latency reversal and immune elimination of persistent HIV-1. *EBioMedicine*. 2019;43:295–306.
20 Kahan SM, Wherry EJ, Zajac AJ. T cell exhaustion during persistent viral infections. *Virology*. 2015;479-480:180–193.
21 Kinloch-de Loes S. Role of therapeutic vaccines in the control of HIV-1. *J Antimicrob Chemother*. 2004;53(4):562–566.
22 Fenwick C, Joo V, Jacquier P, et al. T-cell exhaustion in HIV infection. *Immunol Rev*. 2019;292(1):149–163.
23 Sharpe AH, Pauken KE. The diverse functions of the PD1 inhibitory pathway. *Nat Rev Immunol*. 2018;18(3):153–167.
24 Reiser J, Effector Banerjee A. Memory, and dysfunctional CD8(+) T cell fates in the antitumor immune response. *J Immunol Res*. 2016;2016:8941260.
25 Kallies A, Zehn D, Utzschneider DT. Precursor exhausted T cells: key to successful immunotherapy? *Nat Rev Immunol*. 2020;20(2):128–136.
26 Bengsch B, Johnson AL, Kurachi M, et al. Bioenergetic insufficiencies due to metabolic alterations regulated by the inhibitory receptor PD-1 are an early driver of CD8(+) T cell exhaustion. *Immunity*. 2016;45(2):358–373.
27 He W, Zhang H, Han F, et al. CD155T/TIGIT signaling regulates CD8(+) T-cell metabolism and promotes tumor progression in human gastric cancer. *Cancer Res*. 2017;77(22):6375–6388.
28 Lee MJ, Yun SJ, Lee B, et al. Association of TIM-3 expression with glucose metabolism in Jurkat T cells. *BMC Immunol*. 2020;21(1):48.
29 Jones N, Cronin JG, Dolton G, et al. Metabolic adaptation of human CD4(+) and CD8(+) T-cells to t-cell receptor-mediated stimulation. *Front Immunol*. 2017;8:1516.
30 Ma EH, Bantug G, Griss T, et al. Serine is an essential metabolite for effector T cell expansion. *Cell Metab*. 2017;25(2):345–357.
31 Guo Y, Xie YQ, Gao M, et al. Metabolic reprogramming of terminally exhausted CD8(+) T cells by IL-10 enhances anti-tumor immunity. *Nat Immunol*. 2021;22(6):746–756.
32 Angin M, Volant S, Passaes C, et al. Metabolic plasticity of HIV-specific CD8(+) T cells is associated with enhanced antiviral potential and natural control of HIV-1 infection. *NatMetabol*. 2019;1(7):704–716.
33 Day EA, O'Neill LAJ. Targeting mitochondria to beat HIV-1. *Nat Immunol*. 2021;22(4):398–399.
34 Martin GE, Frater J. Post-treatment and spontaneous HIV control. *Curr Opin HIV AIDS*.. 2018;13(5):402–407.
35 Sáez-Cirión A, Bacchus C, Hocqueloux L, et al. Post-treatment HIV-1 controllers with a long-term virological remission after the interruption of early initiated antiretroviral therapy ANRS VISCONTI study. *PLoS Pathog*. 2013;9(3):e1003211.
36 Horiuchi T, Sakata N, Narumi Y, et al. Metformin directly binds the alarmin HMGB1 and inhibits its proinflammatory activity. *J Biol Chem*. 2017;292(20):8436–8446.
37 Li L, Wang L, Li J, et al. Metformin-induced reduction of CD39 and CD73 blocks myeloid-derived suppressor cell activity in patients with ovarian cancer. *Cancer Res*. 2018;78(7):1779–1791.
38 Zhang Z, Li F, Tian Y, Cao L, et al. Metformin enhances the antitumor activity of CD8(+) T lymphocytes via the AMPK-miR-107-eomes-PD-1 pathway. *J Immunol*. 2020;204(9):2575–2588.
39 Singhal A, Jie L, Kumar P, et al. Metformin as adjunct antituberculosis therapy. *Sci Transl Med*. 2014;6(263).263ra159.
40 Ruiz A, Blanch-Lombarte O, Jimenez-Moyano E, et al. Antigen production after latency reversal and expression of inhibitory receptors in CD8+ T cells limit the killing of HIV-1 reactivated cells. *Front Immunol*. 2018;9:3162.
41 Phan AT, Doedens AL, Palazon A, et al. Constitutive glycolytic metabolism supports CD8(+) T cell effector memory differentiation during viral infection. *Immunity*. 2016;45(5):1024–1037.
42 Cheng L, Wang Q, Li G, et al. TLR3 agonist and CD40-targeting vaccination induces immune responses and reduces HIV-1 reservoirs. *J Clin Invest*. 2018;128(10):4387–4396.
43 Smith KN, Mailliard RB, Piazza PA, et al. Effective cytotoxic T lymphocyte targeting of persistent HIV-1 during antiretroviral therapy requires priming of naive CD8+ T cells. *mBio*. 2016;7(3).
44 Coffman RL, Sher A, Seder RA. Vaccine adjuvants: putting innate immunity to work. *Immunity*. 2010;33(4):492–503.
45 Poteet E, Lewis P, Li F, et al. A novel prime and boost regimen of HIV virus-like particles with TLR4 adjuvant MPLA induces Th1 oriented immune responses against HIV. *PLoS One*. 2015;10(8):e0136862.
46 Phillips B, Van Rompay KKA, Rodriguez-Nieves J, et al. Adjuvant-dependent enhancement of HIV Env-specific antibody responses in infant Rhesus Macaques. *J Virol*. 2018;92(20).
47 Kasturi SP, Rasheed MAU, Havenar-Daughton C, et al. 3M-052, a synthetic TLR-7/8 agonist, induces durable HIV-1 envelope-specific plasma cells and humoral immunity in nonhuman primates. *Sci Immunol*. 2020;5(48).
48 Borducchi EN, Liu J, Nkolola JP, et al. Antibody and TLR7 agonist delay viral rebound in SHIV-infected monkeys. *Nature*. 2018;563(7731):360–364.
49 Liang F, Lindgren G, Sandgren KJ, et al. Vaccine priming is restricted to draining lymph nodes and controlled by adjuvant-mediated antigen uptake. *Sci Transl Med*. 2017;9(393).
50 Plana M, García F, Gallart T, et al. Immunological benefits of antiretroviral therapy in very early stages of asymptomatic chronic HIV-1 infection. *AIDS*. 2000;14(13):1921–1933.
51 Korencak M, Byrne M, Richter E, et al. Effect of HIV infection and antiretroviral therapy on immune cellular functions. *JCI Insight*. 2019;4(12).
52 Sáez-Cirión A, Sereti I. Immunometabolism and HIV-1 pathogenesis: food for thought. *Nat Rev Immunol*. 2021;21(1):5–19.
53 Martin-Gayo E, Yu XG. Dendritic cell immune responses in HIV-1 controllers. *Curr HIV/AIDS Rep*. 2017;14(1):1–7.
54 Boppana S, Goepfert P. *Understanding the CD8 T-Cell Response in Natural HIV Control*. 7. F1000Research; 2018.
55 Velu V, Titanji K, Zhu B, et al. Enhancing SIV-specific immunity in vivo by PD-1 blockade. *Nature*. 2009;458(7235):206–210.
56 Mylvaganam GH, Chea LS, Tharp GK, et al. Combination anti-PD-1 and antiretroviral therapy provides therapeutic benefit against SIV. *JCI Insight*. 2018;3(18).
57 Etemad B, Esmaeilzadeh E, Li JZ. Learning from the exceptions: HIV remission in post-treatment controllers. *Front Immunol*. 2019;10:1749.
58 McMahon J, Lewin SR, Rasmussen TA. Viral, inflammatory, and reservoir characteristics of posttreatment controllers. *Curr Opin HIV AIDS*.. 2021;16(5):249–256.
59 Perdomo-Celis F, Velilla PA, Taborda NA, Rugeles MT. An altered cytotoxic program of CD8+ T-cells in HIV-infected patients despite HAART-induced viral suppression. *PLoS One*. 2019;14(1):e0210540.
60 Buzon MJ, Martin-Gayo E, Pereyra F, et al. Long-term antiretroviral treatment initiated at primary HIV-1 infection affects the size, composition, and decay kinetics of the reservoir of HIV-1-infected CD4 T cells. *J Virol*. 2014;88(17):10056–10065.
61 Keating SM, Jones RB, Lalama CM, et al. Brief report: HIV antibodies decline during antiretroviral therapy but remain correlated with HIV DNA and HIV-specific T-cell responses. *J Acquir Immune Defic Syndr*. 2019;81(5):594–599.
62 Morvan MG, Teque FC, Locher CP, Levy JA. The CD8(+) T cell non-cytotoxic antiviral responses. *Microbiol Mol Biol Rev*. 2021;85(2).
63 Jin JH, Huang HH, Zhou MJ, et al. Virtual memory CD8+ T cells restrain the viral reservoir in HIV-1-infected patients with antiretroviral therapy through derepressing KIR-mediated inhibition. *Cell Mol Immunol*. 2020;17(12):1257–1265.
64 Le Bert N, Gill US, Hong M, et al. Effects of hepatitis B surface antigen on virus-specific and global T cells in patients with chronic hepatitis B virus infection. *Gastroenterology*. 2020;159(2):652–664.
65 Collins DR, Urbach JM, Racenet ZJ, et al. Functional impairment of HIV-specific CD8(+) T cells precedes aborted spontaneous control of viremia. *Immunity*. 2021;54(10):2372–2384.e7.
66 Banga R, Rebecchini C, Procopio FA, et al. Lymph node migratory dendritic cells modulate HIV-1 transcription through PD-1 engagement. *PLoS Pathog*. 2019;15:(7) e1007918.
67 Sperk M, Domselaar RV, Neogi U. Immune checkpoints as the immune system regulators and potential biomarkers in HIV-1 infection. *Int J Mol Sci*. 2018;19(7).

68 Tang R, Rangachari M, Kuchroo VK. Tim-3: a co-receptor with diverse roles in T cell exhaustion and tolerance. *Semin Immunol*. 2019;42:101302.

69 Hudson WH, Gensheimer J, Hashimoto M, et al. Proliferating transitory T cells with an effector-like transcriptional signature emerge from PD-1(+) stem-like CD8(+) T cells during chronic infection. *Immunity*. 2019;51(6):1043–1058.e4.

70 Liu Z, Xiang C, Han M, Meng N, Luo J, Fu R. Study on Tim3 regulation of multiple myeloma cell proliferation via NF-κB signal pathways. *Front Oncol*. 2020;10:584530.

71 Mehraj V, Routy JP. Tryptophan catabolism in chronic viral infections: handling uninvited guests. *Int J Tryptophan Res: IJTR*. 2015;8:41–48.

72 Chen J, Xun J, Yang J, et al. Plasma Indoleamine 2,3-dioxygenase activity is associated with the size of the human immunodeficiency virus reservoir in patients receiving antiretroviral therapy. *Clin Infect Dis*. 2019;68(8):1274–1281.

73 Salminen A. Increased immunosuppression impairs tissue homeostasis with aging and age-related diseases. *J Mol Med*. 2021;99(1):1–20.

74 Ogbechi J, Clanchy FI, Huang YS, Topping LM, Stone TW, Williams RO. IDO activation, inflammation and musculoskeletal disease. *Exp Gerontol*. 2020;131:110820.

75 Rahman AN, Liu J, Mujib S, et al. Elevated glycolysis imparts functional ability to CD8(+) T cells in HIV infection. *Life Sci Alliance*. 2021;4(11).

76 Shytaj IL, Procopio FA, Tarek M, et al. Glycolysis downregulation is a hallmark of HIV-1 latency and sensitizes infected cells to oxidative stress. *EMBO Mol Med*. 2021;13(8):e13901.

77 Utzschneider DT, Charmoy M, Chennupati V, et al. T cell factor 1-expressing memory-like CD8(+) T cells sustain the immune response to chronic viral infections. *Immunity*. 2016;45(2):415–427.

78 Liesa M, Shirihai OS. Mitochondrial networking in T cell memory. *Cell*. 2016;166(1):9–10.

79 Buck MD, O'Sullivan D, Klein Geltink RI, et al. Mitochondrial dynamics controls T cell fate through metabolic programming. *Cell*. 2016;166(1):63–76.

80 Cao W, Mehraj V, Trottier B, et al. Early initiation rather than prolonged duration of antiretroviral therapy in HIV infection contributes to the normalization of CD8 T-cell counts. *Clin Infect Dis*. 2016;62(2):250–257.

81 Gálvez C, Urrea V, Dalmau J, et al. Extremely low viral reservoir in treated chronically HIV-1-infected individuals. *EBioMedicine*. 2020;57:102830.

82 Warren JA, Clutton G, Goonetilleke N. Harnessing CD8(+) T cells under HIV antiretroviral therapy. *Front Immunol*. 2019;10:291.

83 Martin-Cofreces NB, Chichon FJ, Calvo E, et al. The chaperonin CCT controls T cell receptor-driven 3D configuration of centrioles. *Sci Adv*. 2020;6(49).